
MSAFlow: a Unified Approach for MSA Representation, Augmentation, and Family-based Protein Design

Anonymous Author(s)

Affiliation

Address

email

Abstract

1 Multiple Sequence Alignments (MSAs) provide fundamental information about
2 protein evolutionary trajectories and play crucial roles in downstream tasks such as
3 augmentation and family-based design. However, constructing high-quality MSAs
4 requires significant computational resources to query natural protein databases,
5 and traditional techniques fail to provide relevant data for proteins with limited
6 evolutionary information. While deep learning approaches have shown promise
7 in MSA construction and augmentation, they fail to capture rich distributional
8 information while preserving permutation invariance. MSAFlow addresses these
9 limitations using a Statistical Flow Matching model conditioned on compressed
10 latent MSA representations to generate sequences that would likely belong to the
11 target MSA. This approach captures distributional information while augmenting
12 shallow MSAs and maintaining permutation invariance. Experiments confirm that
13 MSAFlow generates MSAs with performance comparable to traditional methods
14 on family-based design tasks. The model outperforms existing machine learning
15 augmentation tools while achieving very low inference time and memory efficiency
16 despite being lightweight and trained on smaller datasets. MSAFlow enables
17 family-based protein design for enzymes and synthetic MSA generation through
18 latent diffusion. Extensive ablation studies validate the effectiveness of model
19 design components. Overall, MSAFlow provides a robust and efficient framework
20 for MSA representation and integration in downstream applications.

21

1 Introduction

22 Multiple Sequence Alignments (MSAs) provide fundamental information about protein evolutionary
23 trajectories and play crucial roles in downstream tasks such as augmentation and family-based design.
24 MSAs represent collections of homologous proteins that delineate the evolutionary history of a single
25 query sequence, enabling models to identify conserved regions and detect evolutionary couplings.
26 Moreover, MSAs carry significant information about functional sites within the query sequence;
27 for instance, comparing sequences across a family of enzymes can reveal conserved active site
28 residues. However, constructing high-quality MSAs requires significant computational resources
29 to query natural protein databases. While traditional statistical search methods such as HHBLits
30 [1], MMSeqs [2], and JackHMMER [3] can accurately identify evolutionarily-related sequences,
31 they incur significant computational costs and traditional techniques fail to provide relevant data for
32 proteins with limited evolutionary information.

33 This challenge has been partially addressed by Dense Homology Retriever (DHR) [4], which leverages
34 pretrained embeddings from protein language models to identify homologous sequences more
35 efficiently and with greater sensitivity. Several other models, including MSAGenerator [5], MSAGPT

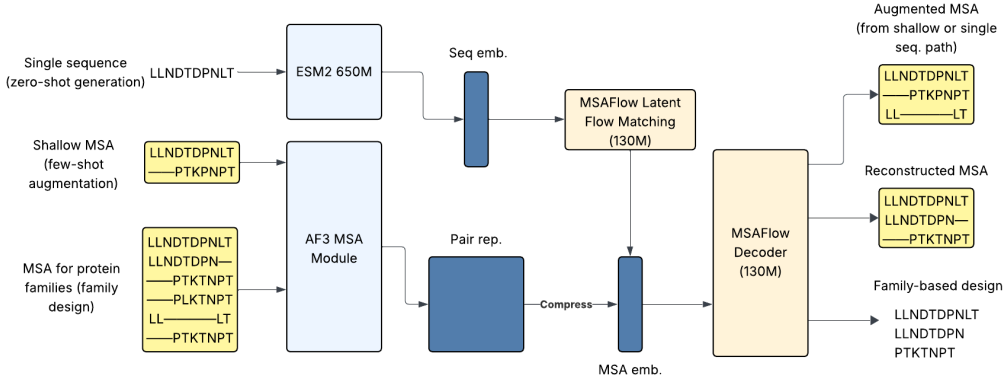


Figure 1: **General framework of MSAFlow.** Our approach supports three complementary pathways: (1) zero-shot generation from a single sequence using ESM2 embeddings, (2) few-shot augmentation of shallow MSAs, and (3) family-based design given MSAs embedded through the AF3 MSA Module and reconstructed through MSAFlow Decoder. All pathways leverage the latent flow-matching and decoder architecture to generate augmented or compressed MSAs, enabling both the enhancement of limited evolutionary information and the efficient representation of deep alignments.

[6], and EvoDiff [7], have subsequently emerged, employing autoregressive or discrete diffusion frameworks to model the joint distribution of multiple sequences in MSAs. While deep learning approaches have shown promise in MSA construction and augmentation, they fail to capture rich distributional information while preserving permutation invariance.

However, these methods typically utilize 2D positional encodings to represent row-wise and column-wise information present in MSAs. These approaches fail in critical aspects: they are substantially memory-intensive due to the $O(N^2)$ space complexity of self-attention operations, further exacerbated by the 2D nature of MSAs, and they lack permutation invariance, naively prioritizing certain sequences without employing permutation-invariant aggregation techniques. Furthermore, current MSA generation models rely solely on existing MSA sequence information for generation, limiting their effectiveness in shallow MSA enhancement.

To address these limitations, we introduce MSAFlow, which addresses these limitations using a Statistical Flow Matching [8] (SFM) model conditioned on compressed latent MSA representations to generate sequences that would likely belong to the target MSA. The MSAFlow framework first employs the AlphaFold3 [9] (AF3) MSAModule to generate a latent MSA embedding, which aggregates protein MSA information into its corresponding pair representation. We further compress this representation into a single-sequence representation through mean pooling across the second dimension. This embedding subsequently serves as conditional information for the Statistical Flow Matching model trained to reconstruct sequences from the original MSA. This approach captures distributional information while augmenting shallow MSAs and maintaining permutation invariance during reconstruction while enabling latent flow matching on the MSA embedding itself.

Experimental results demonstrate that MSAFlow generates MSAs with performance comparable to traditional methods on family-based design tasks. The model outperforms existing machine learning augmentation tools while achieving very low inference time and memory efficiency despite being lightweight and trained on smaller datasets. We evaluate MSAFlow on its ability to reconstruct MSAs from compressed latent representations, testing both the expressivity of the embeddings and the model’s capacity to interpolate across the entire evolutionary space of proteins. Additionally, we utilize MSAFlow to augment existing shallow MSAs and generate synthetic MSAs for single sequences with limited evolutionary data to enhance structure prediction. MSAFlow enables family-based protein design for enzymes and synthetic MSA generation through latent diffusion, providing a robust and efficient framework for MSA representation and integration in downstream applications.

67 **2 Preliminaries**

68 Multiple Sequence Alignments (MSAs) are mathematically represented as $\mathcal{S} = \{s_1, s_2, \dots, s_M\}$
 69 where each sequence $s_i \in \mathcal{A}^L$ consists of amino acids and gaps from alphabet \mathcal{A} , aligned to a
 70 reference sequence s_{ref} of length L . Despite containing hundreds to thousands of sequences, we
 71 hypothesize that the functional and evolutionary information within an MSA can be **compressed into**
 72 **a continuous latent representation** that captures the essential characteristics of the protein family.

73 This compression necessitates a permutation-invariant encoding method to avoid bias from sequence
 74 ordering. Formally, we seek an encoder $h_\phi : \mathcal{S} \rightarrow \mathbb{R}^d$ such that $h_\phi(\mathcal{S}) = h_\phi(\pi(\mathcal{S}))$ for any
 75 permutation π of the sequences in \mathcal{S} . We leverage the AlphaFold3 (AF3) MSAModule architecture,
 76 which provides a computationally efficient framework for embedding evolutionary information [9].
 77 The AF3 MSAModule processes an MSA by computing a position-wise outer product for each
 78 sequence s_i with the reference sequence, resulting in pairwise representations $P_i \in \mathbb{R}^{L \times L \times h_{\text{pair}}}$.
 79 These representations are averaged across all sequences:

$$P_{\text{avg}} = \frac{1}{M} \sum_{i=1}^M P_i \quad (1)$$

80 The averaged representation is then processed through multiple triangle self-attention blocks to
 81 produce a refined pair representation $P_{\text{refined}} \in \mathbb{R}^{L \times L \times H}$. We utilize Protenix [10], a pretrained
 82 variant of AF3, to generate these embeddings for MSAs from the OpenFold dataset [11]. The resulting
 83 pair representation serves as our compressed MSA embedding $m = h_\phi(\mathcal{S}) \in \mathbb{R}^{L \times L \times H}$.

84 **3 Method**

85 **3.1 Flow-matching based autoencoder for MSA representation**

86 **3.1.1 Probabilistic Framework**

87 We view our model as a conditional generator over the sequence distribution of a protein family. Given
 88 an MSA \mathcal{S} and its embedding $m = h_\phi(\mathcal{S})$, the decoder aims to reconstruct sequences consistent with
 89 the family. Let $\tilde{\mathcal{S}} = \{s_1, \dots, s_n\}$ be n sequences drawn uniformly without replacement from \mathcal{S} . We
 90 model

$$p_\theta(\tilde{\mathcal{S}} | m) = \prod_{i=1}^n p_\theta(s_i | m), \quad (2)$$

91 which is permutation-invariant by construction. The decoder $p_\theta(s | m)$ represents the probability of
 92 sampling a sequence s compatible with m .

93 **3.1.2 Statistical Flow Matching for MSA sequence decoding**

94 To instantiate $p_\theta(s | m)$ for discrete (categorical) sequences, we adopt Statistical Flow Matching
 95 (SFM) [12], which learns a continuous Riemannian flow over the statistical manifold of categorical
 96 distributions equipped with Fisher-Rao metric. Concretely, each sequence in the MSA is treated as a
 97 sample of the target distribution. We operate in the probability simplex $\Delta^{|\mathcal{A}| \times L}$, where each position
 98 in the sequence is represented by a one-hot categorical distribution μ over amino acids.

99 Following SFM, we construct flow paths along geodesics on the positive orthant of the unit sphere
 100 by applying the mapping: $\pi : x = \pi(\mu) = \sqrt{\mu}$. SFM demonstrated that such a mapping to the
 101 unit sphere preserves the metric, which coincides with the canonical spherical geometry. Therefore,
 102 we can operate on the unit sphere with the standard spherical geometry. Mathematically, given a
 103 sequence s_i from the MSA and its corresponding categorical representation $x_1 = \pi(\mu_1)$ (e.g., one-hot
 104 encoding) and the noise representation $x_0 = \pi(\mu_0)$, the time-dependent interpolation follows:

$$x_t = \exp_{x_0}(t \cdot \log_{x_0}(x_1)) \quad (3)$$

105 where \exp and \log are the spherical exponential and logarithm maps on the manifold, respectively,
106 and can be calculated in closed form as

$$\exp_x(u) = x \cos \|u\|_2 + \frac{u}{\|u\|_2} \sin \|u\|_2, \quad (4)$$

$$\log_x(y) = \frac{\arccos(\langle x, y \rangle)}{\sqrt{1 - \langle x, y \rangle^2}} (y - x - \langle x, y - x \rangle x), \quad (5)$$

107 After transforming back to the simplex with $\mu_t = \pi^{-1}(x_t)$, the interpolation in Equation 3 traces the
108 geodesic between μ_0 and μ_1 with respect to the Fisher information metric, ensuring we follow the
109 shortest path on the statistical manifold. The corresponding vector field for this mapped geodesic
110 flow is given by:

$$u_t(x_t|x_0, x_1) = \frac{\log_{x_t}(x_1)}{1 - t}. \quad (6)$$

111 Instead of an unconditional model, our MSAFlow decoder employs a conditional parameterization
112 where $v_\theta(x_t|m, t)$ is trained to approximate the vector field conditioning on the MSA embedding
113 $m = h_\phi(\mathcal{S})$:

$$\mathcal{L}_{\text{SFM}}(\theta) = \mathbb{E}_{t \sim \mathcal{U}[0,1], s_i \sim \mathcal{S}, \mu_0 \sim \pi_* p_0, \mu_1 \sim \pi_* \delta(s_i)} [\|v_\theta(x_t|m, t) - u_t(x_t|x_0, x_1)\|^2] \quad (7)$$

114 where π_* denotes the pushward of applying the mapping π , x_t is obtained via the geodesic inter-
115 polation, and $\delta(s_i)$ represents the categorical distribution corresponding to sequence s_i (typically a
116 one-hot encoding) in an MSA. During sampling, we first follow the learned marginal vector field
117 on the sphere to obtain x_1 , then discrete generations of MSAs can be sampled from the categorical
118 distribution $\mu_1 = \pi^{-1}(x_1)$.

119 3.1.3 Model Architecture and Implementation

120 We implement the vector field model
121 v_θ using a modified conditional Di-
122 fusion Transformer (DiT) architec-
123 ture. Since the output of the AF3
124 MSA Module is the pair representa-
125 tion of dimension $L \times L \times H$, we first
126 compress it along the second dimen-
127 sion through mean pooling to obtain
128 a sequence-level representation of di-
129 mension $L \times H$:

$$m_{\text{seq}} = \frac{1}{L} \sum_{j=1}^L m_{:,j,:} \in \mathbb{R}^{L \times H} \quad (8)$$

130 This compressed representation serves
131 as conditional information for the DiT
132 model, which consists of 12 trans-
133 former blocks with a hidden dimen-
134 sion of 768, totaling approximately
135 130M parameters. The architecture
136 incorporates sinusoidal time embed-
137 dings for the diffusion timestep t , to-
138 ken embeddings for each amino acid
139 position, conditional embeddings from the compressed MSA representation, and multi-headed self-
140 attention blocks with adaptive layer normalization. Notably, the MSA embedding conditioning is
141 applied per-residue through a position-wise AdaLN to achieve residue-level control. At inference
142 time, we sample sequences by starting with random noise $x_1 \sim \text{Uniform}(\mathcal{A})$ and iteratively applying:

$$x_{t-\Delta t} = x_t - v_\theta(x_t|m, t) \cdot \Delta t \quad (9)$$

143 for timesteps $t = 1, 1 - \Delta t, 1 - 2\Delta t, \dots, 0$, where Δt is a small step size (typically 0.01). At $t = 0$,
144 we obtain the final sequence by taking the argmax over the amino acid probabilities at each position.

145 **3.2 Conditional latent flow matching for MSA embedding generation**

146 While our decoder model generates sequences from MSA embeddings, we also develop a comple-
147 mentary approach to generate synthetic MSA embeddings themselves. This enables us to create
148 artificial MSAs for proteins with limited evolutionary data (e.g., de novo proteins and antibodies).

149 **3.2.1 Problem Formulation**

150 Let $z_1 = h_\phi(\mathcal{S}) \in \mathbb{R}^{L \times H}$ be the compressed MSA embedding for a reference sequence s_{ref} , and let
151 $e = g_\psi(s_{\text{ref}}) \in \mathbb{R}^{d_e}$ be its ESM embedding. We aim to learn a conditional generative model $p_\theta(z_1|e)$
152 that can produce plausible MSA embeddings given only the reference sequence embedding.

153 **3.2.2 Latent Flow Matching**

154 We train a *conditional rectified flow* that maps a standard Gaussian $z_0 \sim \mathcal{N}(0, I)$ to the distribution
155 of MSA embeddings $p(z | e)$ conditioned on the ESM embedding e . We use a straight-line path
156 $z_t = (1-t)z_1 + t z_0$ from target z_1 (the ground-truth MSA embedding) to noise z_0 , whose reference
157 velocity is the constant field $u_t^*(z_t; z_0, z_1) = z_0 - z_1$. A time-dependent, conditional velocity
158 $v_\theta(z_t, e, t)$ is learned by least-squares flow matching:

$$\mathcal{L}_{\text{RFM}} = \mathbb{E}_{t \sim \mathcal{U}[0,1], z_0 \sim \mathcal{N}(0, I), z_1} \| v_\theta(z_t, e, t) - (z_0 - z_1) \|_2^2,$$

159 which provides a simple, stable objective without explicit score estimation.

160 **3.2.3 Generative Sampling Process**

161 At inference, we draw $z_0 \sim \mathcal{N}(0, I)$ and integrate the learned conditional velocity backward from
162 $t=1$ to $t=0$ with an explicit Euler solver. By default we use the deterministic probability-flow ODE
163 ($T=0$); optionally, we add isotropic noise with temperature $T \in [0, 1]$ to trade fidelity for diversity:

$$z_{t-\Delta t} = z_t - v_\theta(z_t, e, t) \Delta t + T \sqrt{\Delta t} \varepsilon, \quad \varepsilon \sim \mathcal{N}(0, I).$$

164 Empirically, smaller T (e.g., $T < 0.5$) improves alignment to e , while larger T increases sample
165 diversity. Full SDE variants and discretization details follow [13] and are deferred to the Appendix.

166 **3.2.4 End-to-End MSA Generation Pipeline**

167 Our complete framework enables two complementary paths for MSA generation (as shown in Figure
168 1), each tailored to specific protein scenarios:

169 **MSA Compression and Reconstruction:** For deep MSAs with abundant evolutionary information,
170 we first compress the multidimensional sequence information through the AF3 MSAModule into
171 a compact latent representation. This compressed embedding effectively captures the evolutionary
172 and functional signals present in the original MSA. We then use our SFM decoder to selectively
173 reconstruct sequences, maintaining the key evolutionary characteristics while reducing redundancy.

174 **Zero-shot MSA Generation:** For orphan or de novo proteins with limited evolutionary data, we
175 first generate the ESM embedding of the single available sequence. Our latent diffusion model then
176 transforms this single-sequence representation into a synthetic MSA embedding that emulates the
177 evolutionary diversity typically found in natural protein families. Finally, we decode multiple diverse
178 sequences from this embedding using our SFM decoder, effectively bootstrapping evolutionary
179 information where none previously existed.

180 **Family-based Design:** To perform family-based design for enzymes, we first gather all sequences
181 belonging to the enzyme class of a given query. These sequences are compressed into a latent
182 representation using the MSAModule distilled from AF3. Our SFM decoder then generates new
183 sequences conditioned on this latent embedding, effectively producing candidates that are highly
184 likely to belong to the original enzyme class. Because the generated sequences may include gaps, we
185 can support both variable-length and fixed-length design: gaps can be ignored when constructing the
186 final sequence, enabling flexible design strategies.

187 This approach combines both MSA compression and generation capabilities in a unified framework.
188 For data-rich scenarios, our method enables efficient information extraction from deep MSAs while

189 preserving their evolutionary signals. For data-limited proteins, it allows the creation of synthetic
 190 alignments that capture potential evolutionary diversity. The integration of these complementary
 191 pathways addresses a fundamental limitation in protein analysis by extending evolutionary context to
 192 proteins that previously lacked sufficient homologous sequences, potentially improving downstream
 193 structure prediction, functional annotation tasks, and family-based design ability.

194 **4 Experiments**

195 **4.1 Benchmarking MSA Autoencoding**

196 We evaluate the reconstruction ability of our model on 50 proteins released by CAMEO on May 10,
 197 2025, where the ground truth MSA is generated using the same procedure as described in [10]. We
 198 then compute the embedding for each MSA via the AF3 MSAModule, and generate 32 sequences
 199 given each latent MSA representation. We find that the relatively shallow MSAs generated by our
 200 model through this method come close to matching the deep, ground-truth MSAs in terms of pLDDT
 201 (87.8 vs. 91.6) and TM-scores (0.83 vs. 0.89) while only consuming 6.5% of the overall bits required
 202 to represent a deep MSA (this is for an average sequence length of 365 and number of alignments
 203 being more than 7,000 from the CAMEO dataset. We perform conditional generation given an
 204 embedding of 16-bit floats with an average size of 365×128 from the CAMEO dataset).

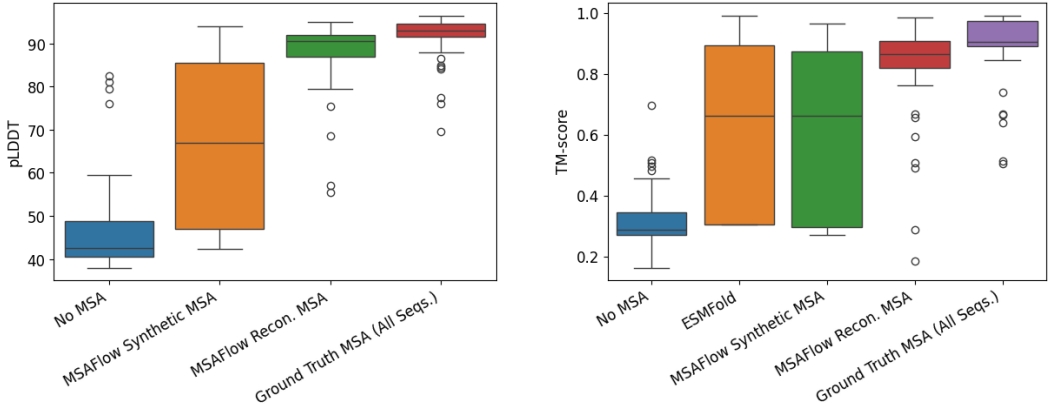


Figure 3: pLDDT and TM-scores for AF3 predictions of proteins from CAMEO with no MSA, the MSAFlow-based reconstructed MSA (32 sequences), a randomly subsampled 32-sequence MSA, and the ground truth deep MSA (approximately 7k sequences).

205 Furthermore, when attempting to build synthetic MSA embedding (i.e. MSAs generated via our
 206 latent diffusion model), we find that our decoder is able to reconstruct some signal from the generated
 207 MSA latents, achieving much higher quality than without using an MSA altogether, although the
 208 structure prediction accuracy remains worse than using the ground truth embedding itself. Another
 209 noteworthy point is that our model effectively compresses the heavy signal of full-depth evolutionary
 210 information encoded in thousands of aligned sequences into a single, fixed-size latent tensor that can
 211 be dynamically decoded into a range of sequences that remain evolutionarily related to the query. As
 212 a result, we keep almost all of the functional signal that matters for folding accuracy.

213 **4.2 Augmenting shallow and single-sequence MSAs**

214 We further evaluate our model on a dataset of sequences with limited evolutionary information
 215 derived from MSAGPT [6], which includes 200 proteins from CAMEO [14], CASP14, CASP15, and
 216 PDB [15] with either few or no sequences in their MSA (few-shot and zero-shot cases, respectively).
 217 For the zero-shot case, we embed the query sequence with ESM and use it as conditioning for our
 218 latent diffusion model, which generates a synthetic MSA embedding for the reference sequence.
 219 We generate embeddings over 10 different seeds and use low temperature sampling during the SDE
 220 forward pass for higher fidelity reconstructions, as detailed in [16]. We then decode 32 sequences
 221 from each of the 10 synthetic MSA embeddings and report the best pLDDT and TM-scores. We find

222 that our model significantly improves upon prior state-of-the-art MSA augmentation tools, which
223 also seemed to yield poorer results when evaluated with AF3.

Table 1: The accuracy of MSAFlow-generated multiple sequence alignments compared to other state-of-the-art methods, as evaluated by AlphaFold3 protein structure prediction performance on a naturally scarce MSA dataset curated from CAMEO, PDB, and CASP.

	pLDDT		TM-score	
	Zero-shot	Few-shot	Zero-shot	Few-shot
No/Shallow MSA	73.1	70.8	0.55	0.58
EvoDiff (650M)	67.7	67.5	0.49	0.55
MSAGPT (3B)	71.6	70.3	0.53	0.58
MSAFlow (Ours,130M)	75.2	70.4	0.62	0.60

224 For the few-shot augmentation case, we use our latent flow matching model to generate synthetic
225 embeddings for each sequence over 5 different seeds, and decode 32 sequences from each MSA
226 embedding. We then decode 64 sequences from the ground-truth shallow MSA embedding and
227 extract the 16 most diverse sequences across all generations, following [6]. We concatenate our
228 generated sequences with the original shallow MSA and find that our model improves upon structure
229 prediction accuracy for such cases.

230 4.3 Case Studies on *de novo* and intrinsically disordered proteins

231 We show that **MSAFlow** markedly improves structure prediction for notoriously difficult proteins by
232 generating high-quality synthetic MSAs. We focus on three challenging cases from a sparse MSA
233 dataset:

- 234 • **8B4K**: the N-terminal domain of Rfa1 complexed with a phosphorylated Ddc2 peptide—only
235 133 residues, with scarce evolutionary relatives.
- 236 • **8GI8**: a Rosetta-designed four-helix bundle with rigid backbone constraints, extraordinary
237 thermal stability ($T_m > 90^\circ\text{C}$), and NMR-validated topology (backbone RMSD = 1.11 Å).
- 238 • **8OKH**: the crystal structure of *Bdellovibrio bacteriovorus* Bd1399.

239 MSAFlow’s synthetic MSAs significantly outperform both MSA-free predictions and those using
240 MSAGPT, which lacks sufficiently precise coevolutionary signals. This highlights MSAFlow’s
241 strengths in addressing two key failure modes: (i) limited sequence homology and (ii) intrinsically
242 flexible or disordered regions—by synthesizing information-rich, high-fidelity MSAs in latent space
243 that modern folding models require.

244 4.4 Family-based Protein Design

245 To better demonstrate the strength of MSAFlow on few-shot generation and generalization to other
246 downstream applications than AF3 prediction, we now provide new results on family-based enzyme
247 design. **Our experiments demonstrate clear and significant advantages of MSAFlow, particularly**
248 **for EC classes with limited sequences**. Following ProfileBFN [17], we generate sequences in a
249 single shot using our model, for enzymes with less than 20 sequences in their corresponding EC
250 class, using the sequences from the EC class as an MSA. We then use CLEAN [18] to determine
251 their EC number, and compute the accuracy (i.e. how many generated designs match the ground
252 truth EC number) and the uniqueness across all generated designs. We report the accuracy \times
253 uniqueness score as done by ProfileBFN, the current SOTA for this task. **MSAFlow exhibits SOTA**
254 **performance on family-based enzyme design in both fixed and variable length settings**. Notably,
255 ProfileBFN is confined to fixed-length generation, whereas MSAFlow learns a meaningful homology
256 distribution that guides the placement of gaps, which effectively enables variable-length design with
257 unprecedented success rate.

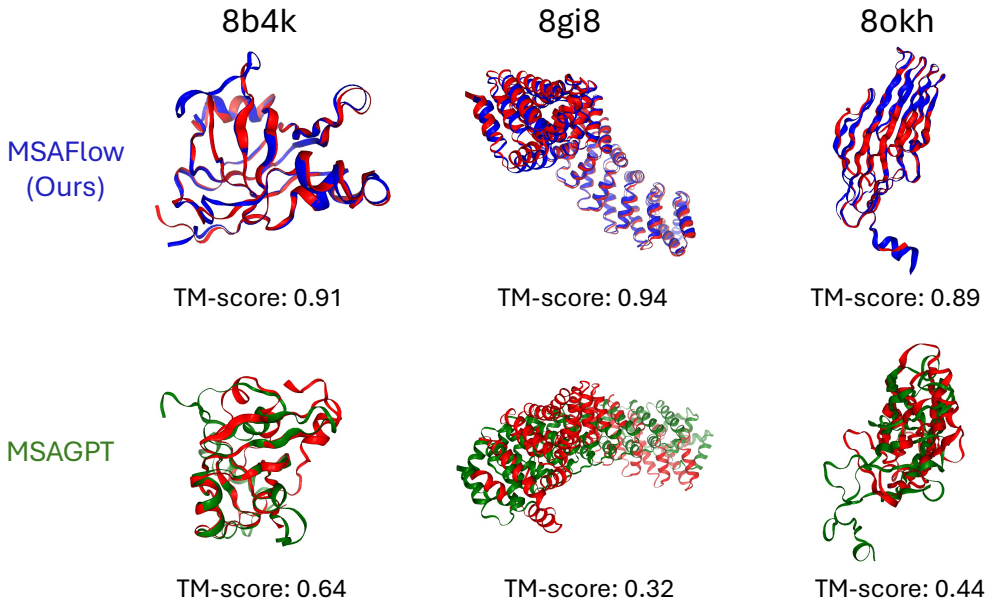


Figure 4: Visualization of improved structure prediction for zero-shot augmentation on de novo and disordered proteins with MSAFlow decoded synthetic MSAs, as compared to MSAs generated with MSAGPT. **Blue** represents predictions with an MSAFlow-generated MSA and **green** represents predictions with an MSAGPT-generated MSA. **Red** indicates the ground truth structure.

		Q15I65	Q15BH7	P13280	P57298
MSA Depth		15	12	13	15
# of Generated Sequences		1000	100	100	100
Accuracy × Uniqueness (Fixed)	EvoDiff	1.39%	0%	80%	5%
	ProfileBFN	42.67%	89%	100%	82%
	MSAFlow	83.10%	84%	100%	95%
Accuracy × Uniqueness (Variable)	EvoDiff	-	0%	0%	0%
	MSAGPT	-	35.59%	37.5%	24.98%
	MSAFlow	-	92%	92%	84%

Table 2: Performance comparison of MSAFlow with baseline methods on family-based enzyme design task across different EC classes.

258 5 Conclusion

259 MSAFlow integrates statistical flow matching with latent space optimization to enable bidirectional
 260 manipulation of multiple sequence alignments. By combining AlphaFold3-inspired permutation-
 261 equivariant embeddings with diffusion-based generation, it uniquely achieves both evolutionary
 262 signal compression and biologically plausible augmentation of sparse alignments. Comprehensive
 263 benchmarking across three critical applications—latent space reconstruction fidelity, shallow MSA
 264 augmentation for protein structure prediction, and synthetic alignment generation for underrepresented
 265 proteins—demonstrates MSAFlow’s superiority, achieving state-of-the-art performance with only
 266 130M parameters. MSAFlow’s ability to generate evolutionarily coherent sequence ensembles creates
 267 new opportunities for designing orphan proteins and tackling de novo structure prediction challenges.
 268 Importantly, our framework also enables family-based design, where latent representations distilled
 269 from enzyme or protein families can guide the generation of sequences that remain faithful to family-
 270 level constraints while still exploring novel sequence diversity. Overall, MSAFlow advances both
 271 computational efficiency and conceptual modeling of protein sequence spaces through flow-based
 272 generation, paving the way for conditional protein engineering, resource-efficient applications, and
 273 family-level design of functional proteins.

274 **References**

275 [1] Michael Remmert, Andreas Biegert, Andreas Hauser, and Johannes Söding. HHblits: lightning-
276 fast iterative protein sequence searching by HMM-HMM alignment. *Nature Methods*, 9(2):173–
277 175, February 2012.

278 [2] Martin Steinegger and Johannes Söding. MMseqs2 enables sensitive protein sequence searching
279 for the analysis of massive data sets. *Nature Biotechnology*, 35(11):1026–1028, November
280 2017.

281 [3] L. Steven Johnson, Sean R. Eddy, and Elon Portugaly. Hidden Markov model speed heuristic
282 and iterative HMM search procedure. *BMC Bioinformatics*, 11(1):431, August 2010.

283 [4] Liang Hong, Zhihang Hu, Siqi Sun, Xiangru Tang, Jiuming Wang, Qingxiong Tan, Liangzhen
284 Zheng, Sheng Wang, Sheng Xu, Irwin King, Mark Gerstein, and Yu Li. Fast, sensitive detection
285 of protein homologs using deep dense retrieval. *Nat. Biotechnol.*, pages 1–13, August 2024.

286 [5] Le Zhang, Jiayang Chen, Tao Shen, Yu Li, and Siqi Sun. MSA generation with seqs2seqs
287 pretraining: Advancing protein structure predictions, 2024.

288 [6] Bo Chen, Zhilei Bei, Xingyi Cheng, Pan Li, Jie Tang, and Le Song. Msagpt: Neural prompting
289 protein structure prediction via msa generative pre-training, 2024.

290 [7] Sarah Alamdari, Nitya Thakkar, Rianne van den Berg, Alex X. Lu, Nicolo Fusi,
291 Ava P. Amini, and Kevin K. Yang. Protein generation with evolutionary diffu-
292 sion: sequence is all you need. Publisher: Cold Spring Harbor Laboratory _eprint:
293 <https://www.biorxiv.org/content/early/2023/09/12/2023.09.11.556673.full.pdf>.

294 [8] Chaoran Cheng, Jiahua Li, Jian Peng, and Ge Liu. Categorical flow matching on statistical
295 manifolds, 2025.

296 [9] Josh Abramson, Jonas Adler, Jack Dunger, Richard Evans, Tim Green, Alexander Pritzel,
297 Olaf Ronneberger, Lindsay Willmore, Andrew J Ballard, Joshua Bambrick, Sebastian W
298 Bodenstein, David A Evans, Chia-Chun Hung, Michael O'Neill, David Reiman, Kathryn
299 Tunyasuvunakool, Zachary Wu, Akvilé Žemgulytė, Eirini Arvaniti, Charles Beattie, Ottavia
300 Bertolli, Alex Bridgland, Alexey Cherepanov, Miles Congreve, Alexander I Cowen-Rivers,
301 Andrew Cowie, Michael Figurnov, Fabian B Fuchs, Hannah Gladman, Rishabh Jain, Yousaf A
302 Khan, Caroline M R Low, Kuba Perlin, Anna Potapenko, Pascal Savy, Sukhdeep Singh, Adrian
303 Stecula, Ashok Thillaisundaram, Catherine Tong, Sergei Yakneen, Ellen D Zhong, Michal
304 Zieliński, Augustin Žídek, Victor Bapst, Pushmeet Kohli, Max Jaderberg, Demis Hassabis, and
305 John M Jumper. Accurate structure prediction of biomolecular interactions with AlphaFold 3.
306 *Nature*, 630(8016):493–500, June 2024.

307 [10] ByteDance AML AI4Science Team, Xinshi Chen, Yuxuan Zhang, Chan Lu, Wenzhi Ma, Jiaqi
308 Guan, Chengyue Gong, Jincai Yang, Hanyu Zhang, Ke Zhang, Shenghao Wu, Kuangqi Zhou,
309 Yanping Yang, Zhenyu Liu, Lan Wang, Bo Shi, Shaochen Shi, and Wenzhi Xiao. Proteinix
310 - advancing structure prediction through a comprehensive alphafold3 reproduction. *bioRxiv*,
311 2025.

312 [11] Gustaf Ahdritz, Nazim Bouatta, Christina Floristean, Sachin Kadyan, Qinghui Xia, William
313 Gerecke, Timothy J. O'Donnell, Daniel Berenberg, Ian Fisk, Niccolò Zanichelli, Bo Zhang,
314 Arkadiusz Nowaczynski, Bei Wang, Marta M. Stepniewska-Dziubinska, Shang Zhang, Adegoke
315 Ojewole, Murat Efe Guney, Stella Biderman, Andrew M. Watkins, Stephen Ra, Pablo Ribalta
316 Lorenzo, Lucas Nivon, Brian Weitzner, Yih-En Andrew Ban, Shiyang Chen, Minjia Zhang,
317 Conglong Li, Shuaiwen Leon Song, Yuxiong He, Peter K. Sorger, Emad Mostaque, Zhao
318 Zhang, Richard Bonneau, and Mohammed AlQuraishi. Openfold: retraining alphafold2 yields
319 new insights into its learning mechanisms and capacity for generalization. *Nature Methods*,
320 21(8):1514–1524, May 2024.

321 [12] Chaoran Cheng, Jiahua Li, Jian Peng, and Ge Liu. Categorical flow matching on statistical
322 manifolds. *arXiv preprint arXiv:2405.16441*, 2024.

323 [13] Tomas Geffner, Kieran Didi, Zuobai Zhang, Danny Reidenbach, Zhonglin Cao, Jason Yim,
324 Mario Geiger, Christian Dallago, Emine Kucukbenli, Arash Vahdat, and Karsten Kreis. Proteina:
325 Scaling flow-based protein structure generative models, 2025.

326 [14] Jürgen Haas, Alessandro Barbato, Dario Behringer, Gabriel Studer, Steven Roth, Martino
327 Bertoni, Khaled Mostaguir, Rafal Gumienny, and Torsten Schwede. Continuous automated
328 model EvaluatiOn (CAMEO) complementing the critical assessment of structure prediction in
329 CASP12. *Proteins*, 86:387–398, March 2018.

330 [15] H M Berman, J Westbrook, Z Feng, G Gilliland, T N Bhat, H Weissig, I N Shindyalov, and P E
331 Bourne. The protein data bank. *Nucleic Acids Res.*, 28(1):235–242, January 2000.

332 [16] Tomas Geffner, Kieran Didi, Zuobai Zhang, Danny Reidenbach, Zhonglin Cao, Jason Yim,
333 Mario Geiger, Christian Dallago, Emine Kucukbenli, Arash Vahdat, and Karsten Kreis. Proteina:
334 Scaling flow-based protein structure generative models, 2025.

335 [17] Jingjing Gong, Yu Pei, Siyu Long, Yuxuan Song, Zhe Zhang, Wenhao Huang, Ziyao Cao, Shuyi
336 Zhang, Hao Zhou, and Wei-Ying Ma. Steering protein family design through profile bayesian
337 flow. February 2025.

338 [18] Tianhao Yu, Haiyang Cui, Jianan Canal Li, Yunan Luo, Guangde Jiang, and Huimin Zhao.
339 Enzyme function prediction using contrastive learning. *Science*, 379(6639):1358–1363, March
340 2023.

341 **A Additional results**342 **A.1 Zero-shot Prediction Comparison with ESMFold**

Table 3: The accuracy of MSAFlow-generated multiple sequence alignments compared to ESMFold, evaluated on zero-shot protein structure prediction performance on a naturally scarce MSA dataset curated from CAMEO, PDB, and CASP.

	TM-score	
	Zero-shot	Few-shot
No/Shallow MSA	0.55	0.58
EvoDiff (650M)	0.49	0.55
MSAGPT (3B)	0.53	0.58
MSAFlow (Ours,130M)	0.62	0.60
ESMFold	0.58	NA

343 We further compared MSAFlow with ESMFold and other MSA generation models according to
 344 the TM-score after folding. The protein structure prediction research based on MSAFlow has
 345 demonstrated substantial results. Through evaluation on a naturally scarce MSA dataset, the results
 346 show that MSAFlow (applying only 130M parameters) achieved the optimal TM-scores in both
 347 zero-shot and few-shot scenarios, with scores of 0.62 and 0.60 respectively. In comparison, ESMFold
 348 scored 0.58 in zero-shot testing, while competing models such as EvoDiff (650M parameters)
 349 and MSAGPT (3B parameters) performed less effectively than MSAFlow. These results indicate
 350 MSAFlow’s precise modeling in MSA generation and its computational efficiency.

351 **A.2 Additional Case Studies**

352 To further validate the robustness of MSAFlow’s zero-shot predictions, we provide more cases for
 353 comparison. From the table 4, we can observe that MSAFlow achieves improvement on cases with
 354 different structural patterns as well as different families.

PDB ID	Length	Description	GT	MSAGPT	MSAFlow
6NW8_A	27	Scorpion venom toxin	0.39	0.40	0.53
6WKK_X	280	Phage capsid	0.28	0.27	0.55
7EQB_B	80	Central spindle assembly	0.65	0.58	0.71
7QRR_L	153	Noumeavirus	0.31	0.61	0.83
7ZOL_A	151	Cas 7-11 regulator	0.33	0.34	0.67

Table 4: Performance comparison of MSAFlow with baseline methods on clinically relevant proteins showing TM-Score improvements across different structural patterns and protein families.

355 **A.3 Inference Speed and Memory Cost**

356 In order to demonstrate that MSAFlow exhibits notable improvements in sampling efficiency com-
 357 pared to other MSA-based generative models, We benchmark MSAFlow against existing tools,
 358 attempting to generate 100 sequences conditioned on an existing MSA with 6 sequences on an
 359 NVIDIA A40 GPU, and observe the following:

	Latency Per Sequence	Memory Consumption
MSAFlow	1.02s	5.8 GiB
ProfileBFN	8.49s	7.7 GiB
MSAGPT	62.46s	41.6 GiB
EvoDiff	478.24s	4.0 GiB

Table 5: Sampling efficiency comparison of MSAFlow with baseline methods showing latency per sequence and memory consumption on NVIDIA A40 GPU for generating 100 sequences conditioned on an MSA with 6 sequences.

360 We find that MSAFlow has better sampling efficiency, both in terms of speed and memory. We can
361 attribute this to the fact that our model only has to deal with $L \times H$ embedding of the MSA, rather
362 than carry the quadratic cost of representing an MSA in the ambient space. The result shows that
363 MSAFlow has the potential to be a highly light-weight and accurate MSA designer.

364 Moreover, our pipeline utilizes outputs from tools like MMseqs and HMMER for Multiple Sequence
365 Alignment (MSA) reconstruction. A key advantage of this approach is its ability to generate high-
366 quality MSAs even when these standard homology search methods fail to find sufficient homologous
367 information. To provide a quantitative comparison of computational cost, we evaluated our MSAFlow
368 model against HMMER and MMseqs2 for generating an MSA from a single query sequence (PDB
369 9BCZ_A from CAMEO, 644 amino acids). The empirical results are detailed below.

Method	Wall Clock Time (s)
MSAFlow (100 seqs)	153.93
HMMER	310.92
MMseqs2	497.73

Table 6: Computational cost comparison for generating MSA from query sequence alone (PDB 9BCZ_A from CAMEO, 644 AA) showing wall clock time in seconds.

370 These results show that MSAFlow achieves over $2 \times$ speedups compared to HMMER and MMseqs2,
371 while still providing the ability to operate in settings where homology search fails. This confirms that
372 MSAFlow not only addresses the coverage gap but also offers computational efficiency advantages
373 over traditional methods.

374 **A.4 Ablation Study of Reconstruction Sequences**

375 We address using the additional ablation study on the reconstruction task with 2, 4, 8, 16, and 32
376 decoded MSA sequences, as well as the comparison with natural-MSA depth on 3 samples from the
377 CAMEO reconstruction test set.
378 When we keep 2-4 sequences, the MSAFlow reconstructions beat the random ground-truth subsample.
379 As we generate more sequences, the designed MSAs generally match that of the ground-truth samples
380 (AlphaFold3 searched MSA), indicating that MSAFlow accurately captures structure patterns of
381 protein families.

	PDB ID	2	4	8	16	32
Ground Truth Random Sample	9EJY	0.59	0.55	0.85	0.80	0.86
	9BIX	0.19	0.32	0.35	0.32	0.49
	9CVV	0.35	0.31	0.93	0.97	0.98
MSAFlow Reconstruction	9EJY	0.61	0.61	0.84	0.83	0.84
	9BIX	0.28	0.22	0.20	0.30	0.26
	9CVV	0.43	0.62	0.87	0.87	0.97

Table 7: Ablation study comparing MSAFlow reconstruction performance against ground truth random samples across different sequence counts on CAMEO reconstruction test set. Values represent performance metrics for MSA reconstruction quality. Numbers in the first row denotes the amounts of decoding MSA sequences.

382 **A.5 Ablation Study on Synthetic and Reconstructed MSAs**

383 The reconstruction pathway preserves the authentic signal from a limited, shallow MSA, while the
384 latentflow pathway generates evolutionary diversity generalized from other MSA-rich proteins. These
385 two tracks provide complementary signals that make the few-shot augmentation stronger. To provide
386 evidence for this, we detail the separate contributions of each track below:

387 As shown in the table, the reconstruction path focuses on preserving crucial motif information within
388 the limited observed sequences, which is reflected in the lower entropy signals in the shallow MSA.
389 In contrast, the latentflow path generates synthetic MSAs that provide evolution-consistent diversity,
390 resulting in higher entropy.

Few-shot task	TM Score	Avg Per-position Entropy
Syn-16	0.54	2.23
Rec-16	0.52	1.33
Syn+Rec-32	0.57	2.69
Syn+Rec+GT	0.60	2.58
MSAGPT+GT	0.58	1.33
GT	0.58	2.16

Table 8: Ablation study showing the complementary contributions of synthetic and reconstructed MSA pathways in few-shot tasks, demonstrating improved TM scores and entropy characteristics. **Syn** represents Synthetic MSAs; **Rec** represents Reconstructed MSAs. The number denotes amount of MSA sequences.

391 The combination of both tracks leads to an improvement in TM score and an increase in entropy. This
 392 observation confirms that the two tracks offer complementary signals, which synergistically improve
 393 quality. Finally, by augmenting the shallow ground truth MSA with the combined generation output,
 394 we improve prediction accuracy and achieve a better TM score than the MSAGPT baseline, which
 395 is what we report in Table 1. As can be seen, MSAFlow is the only method to achieve a better TM
 396 score than the ground truth, with an entropy value closest to it.

397 **A.6 Ablation Study on ESM Embeddings**

398 To clarify the individual contributions of the ESM embeddings and our proposed Statistical Flow-
 399 matching decoding mechanism, we provide ablation results for the MSAFlow zero-shot track trained
 400 to condition on the one-hot query sequence instead of the ESM embedding:

Method	TM Score
MSAGPT (3B)	0.53
MSAFlow Latent w/ one-hot (130M)	0.55
MSAFlow Latent w/ ESM2 (130M)	0.62

Table 9: Ablation study comparing the contribution of ESM embeddings versus one-hot sequence encoding in MSAFlow’s zero-shot MSA augmentation performance.

401 The results demonstrate that the efficiency of our method. Moreover, ESM2 encoding provides more
 402 useful signals to address the evolutionary information.